# Transmission Matrix Model of a Quarter-Wave-Tube with Gas Temperature Gradients

**Carl Howard**

School of Mechanical Engineering, University of Adelaide, South Australia, Australia

## ABSTRACT

A transmission matrix (also known as four pole) model is presented of a duct with anechoic terminations and a quarter-wave-tube, where each duct segment has a linear temperature gradient. The results from simulations conducted using the mathematical model show good agreement with results from finite element simulations using Ansys. Expressions are derived for the four pole analysis method that are relevant when conducting finite element simulations where an incident acoustic particle velocity is specified as the excitation source. A static thermal finite element analysis is conducted using thermal solid elements to determine the nodal temperatures. The nodal temperatures are transferred to the nodes of the acoustic elements and a harmonic analysis is conducted to determine the pressure within the duct.

## INTRODUCTION

The four pole or transmission matrix method can be used to analyse the one-dimensional acoustical response of duct networks. Many acoustic references describe transmission matrices of ducts where the gas temperature is constant throughout the duct. When the gas temperature varies along the duct, as is the case in many practical exhaust systems, the speed of sound and density of the gas changes with temperature and therefore the acoustic impedance also changes. It has been suggested that small temperature variations can be neglected when predicting the acoustic performance of mufflers (Munjal (1987), p286, Section 8.2), but large temperature differences cannot be ignored.

This paper describes a theoretical model, using the four-pole transmission matrix method, of a duct with anechoic terminations and a quarter-wave tube (QWT) where there are linear temperature gradients along each duct segment.

A finite element model was created using the software Ansys of a duct with anechoic end conditions and a quarter-wave-tube. A capability introduced in Ansys release 14.5 is the ability to define acoustic elements that have temperatures defined at nodes. In previous releases, a set for material properties defined the constant speed of sound and constant density of the gas. A model of a duct with gas temperature variations could only be achieved using short connected duct segments with constant material properties in each segment. Hence, an impedance discontinuity would have been created at the interface between duct segments that had dissimilar material properties, and a propagating acoustic wave would be reflected at the change in acoustic impedance. The new capability enables one to define a temperature gradient across an element so that there is no sudden impedance discontinuity.

An example is shown of the analysis of a duct with anechoic end conditions and a quarter-wave tube, where there are linear temperature gradients in each duct segment. Results from theoretical and finite element models compare favourably.

### Previous Work

Several researchers derived approximate solutions to describe the one-dimensional acoustic response of a duct due to a linear temperature gradient, where there are small temperature differences between the ends of the duct (Munjal & Prasad (1986), Peat (1988)). However these solutions are inaccurate when there are large temperature differences between the ends of the duct. Sujith et al. (1985) derived the exact solution when there are large temperature gradients. Sujith (1996) used the results to derive the four pole transmission matrix form of these equations. Howard (2013) found errors in these equations and presented the corrected equations that are used here to predict the response of a duct with anechoic end conditions and a quarter-wave tube (QWT) where there are temperature gradients within each duct segment.

### List of Symbols

| | |
|---|---|
| $c_1, c_2$ | speed of sound at each end of the duct |
| $j$ | unit imaginary number |
| $J_n$ | Bessel function of the nth order |
| $k$ | wave-number |
| $L$ | length of the duct |
| $M$ | molecular weight of air |
| $N_n$ | Neumann function of the *n*th order |
| $p_1, p_2$ | pressure at the ends of the duct |
| $P_{\text{static}}$ | static pressure in the duct |
| $R$ | universal gas constant |
| $R_s = R/M$ | specific gas constant |
| $S$ | cross sectional area of the duct |
| $T$ | temperature of the fluid |
| $T_1, T_2$ | temperatures of fluid at the ends of the duct |
| $T_{11}, T_{12}, T_{21}, T_{22}$ | elements of a transmission matrix |
| $u_1, u_2$ | particle velocities at the ends of the duct |
| $V_1, V_2$ | mass volume velocity at the ends of the duct |
| $Y, Y_n$ | characteristic impedance |
| $z$ | axial coordinate along the duct |
| $\rho_1, \rho_2$ | density of fluid at ends of duct |
| $\omega$ | angular frequency |
| $\upsilon$ | constant defined in Eq. (18) |
| $\gamma$ | ratio of specific heats ($C_P/C_V$) |

## TRANSMISSION MATRIX MODEL

### Constant Gas Temperature

The acoustic pressure and mass volume velocity at each end of a straight duct segment with a uniform gas temperature is given by (Beranek and Ver (1992), p377, Eq. (10.14))

$$\begin{bmatrix} p_2 \\ V_2 \end{bmatrix} = \begin{bmatrix} T_{11} & T_{12} \\ T_{21} & T_{22} \end{bmatrix} \begin{bmatrix} p_1 \\ V_1 \end{bmatrix} \quad (1)$$

where $V = \rho S u$ is the mass volume velocity. The four pole matrix is

$$\mathbf{T} = \begin{bmatrix} T_{11} & T_{12} \\ T_{21} & T_{22} \end{bmatrix} \quad (2)$$

$$T_{11} = \cos(kL) \quad (3)$$

$$T_{12} = \mathrm{j}\,\frac{c}{S}\sin(kL) \quad (4)$$

$$T_{21} = \mathrm{j}\,\frac{S}{c}\sin(kL) \quad (5)$$

$$T_{22} = \cos(kL) \quad (6)$$

where $k = 2\pi f/c$ is the wave-number, $f$ is the frequency, $c$ is the speed of sound, $L$ is the length of the duct segment. The speed of sound of the gas varies with temperature as (Bies and Hansen (2009), p17, Eq. 1.8)

$$c = \sqrt{\frac{\gamma R T}{M}} \quad \mathrm{m/s} \quad (7)$$

where the properties for air are $\gamma = 1.4$ is the ratio of specific heats, $R = 8.3144621$ J.mol$^{-1}$.K$^{-1}$ is the universal gas constant, $M = 0.029$ kg.mol$^{-1}$ is the molar mass of air, and $T$ is the temperature of the gas in Kelvin. The density of the gas is calculated as (Bies and Hansen (2009), Eq. 1.8, p17-18)

$$\rho = \frac{M P_{\text{static}}}{RT} \quad \mathrm{kg/m^3} \quad (8)$$

where $P_{\text{static}} = 101325$ Pa atmospheric pressure (assuming the gas in the tube is not pressurised).

### Linear Temperature Gradient

This section describes the equations for the four pole matrix of a duct with a linear temperature gradient as presented in Sujith (1996) and the corrected form of the equations presented in Howard (2013).

Consider a duct where there is a temperature gradient of the gas in the duct as shown in Figure 1.

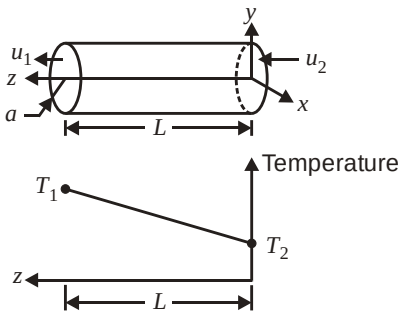


**Figure 1**. Configuration of a duct where the gas has a linear temperature gradient between the inlet and outlet.

The gas at the inlet of the duct has a temperature $T_2$, pressure $p_2$, density $\rho_2$, and particle velocity $u_2$. Similar parameter definitions apply at the outlet of the duct where the parameters have subscript 1. The linear gas temperature profile is

$$T(z) = mz + T_2 \quad (9)$$

where the temperature gradient is defined as

$$m = \frac{T_1 - T_2}{L} \quad (10)$$

Hence, the gas temperature at the inlet is $T(0) = T_2$ and at the outlet is $T(L) = T_1$.

The four pole matrix presented in Sujith (1996) is in terms of the pressure and acoustic particle velocity. The four pole matrix can be modified into terms for pressure and mass volume velocity, to be consistent with expression in Beranek and Ver (1992), p373, and Munjal (1987), Section 2.18, p75, by multiplying the bottom row of the matrix equation on each side by $\rho_2 S_2$ and becomes

$$\begin{bmatrix} p_2 \\ \rho_2 S_2 u_2 \end{bmatrix} = \begin{bmatrix} p_2 \\ V_2 \end{bmatrix} = \begin{bmatrix} T_{11} & T_{12} \\ \rho_2 S_2 T_{21} & \rho_2 S_2 T_{22} \end{bmatrix} \begin{bmatrix} p_1 \\ u_1 \end{bmatrix} \quad (11)$$

and multiplying the bottom row right-hand side of the matrix by $\rho_1 S_1/\rho_1 S_1 = 1$ and rearranging to

$$\begin{bmatrix} p_2 \\ V_2 \end{bmatrix} = \begin{bmatrix} T_{11} & \left[\frac{1}{\rho_1 S_1}\right] T_{12} \\ (\rho_2 S_2)\, T_{21} & \left[\frac{\rho_2 S_2}{\rho_1 S_1}\right] T_{22} \end{bmatrix} \begin{bmatrix} p_1 \\ \rho_1 S_1 u_1 \end{bmatrix} = \begin{bmatrix} p_1 \\ V_1 \end{bmatrix} \quad (12)$$

The elements of the transmission matrix are (Howard (2013))

$$\mathbf{T} = \begin{bmatrix} T_{11} & T_{12} \\ T_{21} & T_{22} \end{bmatrix} \quad (13)$$

$$T_{11} = \left[\frac{\pi\omega\sqrt{T_1}}{\upsilon}\right] \times \left[J_1\left(\frac{\omega\sqrt{T_1}}{\upsilon}\right) N_0\left(\frac{\omega\sqrt{T_2}}{\upsilon}\right) - J_0\left(\frac{\omega\sqrt{T_2}}{\upsilon}\right) N_1\left(\frac{\omega\sqrt{T_1}}{\upsilon}\right)\right] \quad (14)$$

$$T_{12} = 1j \times \left[\frac{\pi\omega\sqrt{T_1}}{\upsilon}\right] \times \left[\frac{|m|}{m}\right] \times \left[\rho_1\sqrt{\gamma R_s T_1}\right] \times \left[J_0\left(\frac{\omega\sqrt{T_2}}{\upsilon}\right) N_0\left(\frac{\omega\sqrt{T_1}}{\upsilon}\right) - J_0\left(\frac{\omega\sqrt{T_1}}{\upsilon}\right) N_0\left(\frac{\omega\sqrt{T_2}}{\upsilon}\right)\right] \quad (15)$$

$$T_{21} = 1j \times \left[\frac{\pi\omega\sqrt{T_1}}{\upsilon}\right] \times \left[\frac{m}{|m|}\right] \times \left[\frac{1}{\rho_2\sqrt{\gamma R_s T_2}}\right] \times \left[J_1\left(\frac{\omega\sqrt{T_2}}{\upsilon}\right) N_1\left(\frac{\omega\sqrt{T_1}}{\upsilon}\right) - J_1\left(\frac{\omega\sqrt{T_1}}{\upsilon}\right) N_1\left(\frac{\omega\sqrt{T_2}}{\upsilon}\right)\right] \quad (16)$$

$$T_{22} = \left[\frac{\pi\omega\sqrt{T_1}}{\upsilon}\right] \times \left[\frac{\rho_1\sqrt{\gamma R_s T_1}}{\rho_2\sqrt{\gamma R_s T_2}}\right] \times \left[J_1\left(\frac{\omega\sqrt{T_2}}{\upsilon}\right) N_0\left(\frac{\omega\sqrt{T_1}}{\upsilon}\right) - J_0\left(\frac{\omega\sqrt{T_1}}{\upsilon}\right) N_1\left(\frac{\omega\sqrt{T_2}}{\upsilon}\right)\right] \quad (17)$$

where the constant $\upsilon$ is

$$\upsilon = \frac{|m|}{2}\sqrt{\gamma R_s} \quad (18)$$

### Transmission Matrices for a Duct with a Quarter Wave Tube

A duct with anechoic terminations and a quarter-wave-tube is shown in Figure 2. The equivalent four pole transmission matrix formulation is shown in Figure 3, where the transmission matrices are $\mathbf{T}_0$ for the outlet termination impedance (an anechoic condition), $\mathbf{T}_1$ for the outlet (downstream) duct, $\mathbf{T}_2$ for the QWT, $\mathbf{T}_3$ for the inlet (upstream) duct.

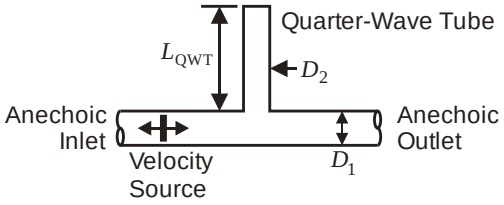


**Figure 2**. Schematic of duct with anechoic inlet and outlet terminations and quarter-wave tube.


**Figure 3.** Four-pole transmission matrix model of the duct system.

The general transmission matrix formulation of a duct system is shown in **Figure 4** (starting from the outlet and traversing upstream) is a load impedance $Z_0$ followed by $n$ transmission matrices, where the inlet pressure $p_n$ and mass volume velocity $V_n$ are applied by an acoustic source. In the example described later, the acoustic excitation used is a volume velocity source $V_s$ and has a source impedance $Z_{n+1}$.

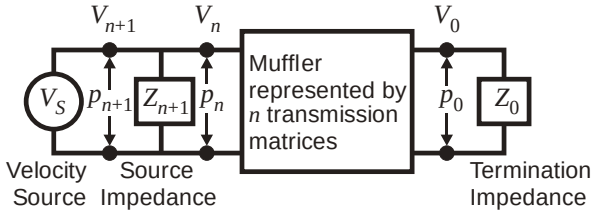


**Figure 4.** Transmission matrix model of a muffler.

The transmission matrix formulation for the system can be written as

$$\begin{bmatrix} p_{\text{inlet}} \\ V_{\text{inlet}} \end{bmatrix} = \mathbf{T}_3\mathbf{T}_2\mathbf{T}_1\mathbf{T}_0 \begin{bmatrix} 0 \\ V_0 \end{bmatrix} \quad (19)$$

$$\begin{bmatrix} p_{\text{inlet}} \\ V_{\text{inlet}} \end{bmatrix} = \begin{bmatrix} E_{11} & E_{12} \\ E_{21} & E_{22} \end{bmatrix} \begin{bmatrix} 0 \\ V_0 \end{bmatrix} \quad (20)$$

where $\mathbf{T}_3, \mathbf{T}_1$ are the transmission matrices for the upstream and downstream duct segments, respectively that are given by Eq. (13). A quarter-wave tube can be considered as a branch impedance and has a transmission matrix given by (Beranek and Ver (1992), p379, Eq. (10.20), Munjal (1987), p80, Eq. (2.148))

$$\mathbf{T_2} = \begin{bmatrix} 1 & 0 \\ \left[\frac{1}{Z_r}\right] & 1 \end{bmatrix} \quad (21)$$

where $Z_r$ is the impedance of the quarter-wave tube, which has the same impedance as a tube with a closed end. The impedance of a quarter-wave tube with a constant gas temperature is given by (Beranek and Ver (1992), p380)

$$Z_r = -j\frac{c}{S}\cot(kL_{\text{QWT}}) \quad (22)$$

The impedance of a quarter wave tube with a linear temperature gradient between the inlet and the closed end can be derived from Eq. (12), by setting the mass volume velocity at the closed end $V_1 = 0$, and calculating the input impedance as

$$Z_r = \frac{p_2}{V_2} = \frac{T_{11}}{T_{21}} \quad (23)$$

where $T_{11}$ is defined in Eq. (14) and $T_{21}$ is defined in Eq. (16). The transmission matrix for the termination impedance, shown as $Z_0$ in Figure 4 can be written as (Munjal (1987), Eq. (2.146), p79) as

$$\begin{bmatrix} p_0 \\ V_0 \end{bmatrix} = \mathbf{T}_0 \begin{bmatrix} 0 \\ V_0 \end{bmatrix} = \begin{bmatrix} 1 & Z_0 \\ 0 & 1 \end{bmatrix} \begin{bmatrix} 0 \\ V_0 \end{bmatrix} \quad (24)$$

and the pressure at the outlet is calculated as

$$p_0 = Z_0 V_0 \quad (25)$$

At this point in the derivation, Eq. (20) can be used to calculate the response of the duct, once the acoustic excitation is known. When conducting Ansys simulations, one can define acoustic excitation sources using several methods. In the example that follows, this is achieved by defining a normal surface velocity at the inlet. However, Eq. (20) is in terms of the total mass volume velocity, which is the sum of the incident and reflected velocities. The following discussion describes how the total mass volume velocity can be determined from the incident mass volume velocity.

The simulations using Ansys involve the application of an incident acoustic particle velocity at the inlet to the duct where there is a super-imposed anechoic boundary condition. Figure 5 shows the configuration of the inlet acoustic excitation.

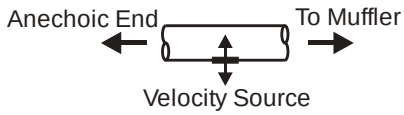


**Figure 5.** Inlet of the duct showing the acoustic velocity source and anechoic termination.

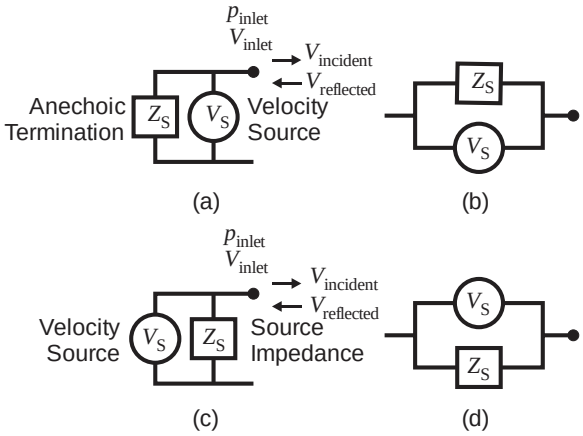


**Figure 6**. Equivalent representations of the acoustic source $V_s$ and source impedance $Z_s$.

The commonly used method in four pole analyses is to specify a total acoustic volume velocity source that is modified by the source impedance. A volume velocity acoustic source could be modelled as a circuit with a branch impedance $Z_s$ (=$Z_{n+1}$) as shown in Figure 6 (a). This circuit is equivalent to Figure 6 (c), which is the representation shown in acoustic references (Munjal (1987), p54, Fig 2.5b). This can be illustrated by considering that Figure 6 (b) is an identical circuit to Figure 6 (a), where the position of the objects have been rotated clockwise by 90 degrees. Similarly Figure 6 (d) is an identical circuit to Figure 6 (c) where the positions of the objects have been rotated clockwise 90 degrees. The circuits in Figure 6 (b) and Figure 6 (d) are identical and hence the circuits in Figure 6 (a) and Figure 6 (c) are identical.

The total acoustic pressure at the *n*th location can be defined as the summation of forward (downstream or incident) travelling waves $A_n$ and backwards (upstream or reflected) travelling waves $B_n$ (Munjal (1987), p81)

$$p_n = A_n + B_n \quad (26)$$

The corresponding total mass volume velocity at the location is defined as

$$V_n = \frac{A_n}{Y_n} + \frac{B_n}{Y_n} \quad (27)$$

where $Y_n = c_n/S_n$ is the characteristic impedance (and should not be confused with acoustic admittance), $c_n$ is the speed of sound at the *n*th location, and $S_n$ is the area of the duct at the *n*th location. When conducting a simulation using Ansys where the normal surface velocity is defined as the acoustic excitation source, one is effectively specifying the incident acoustic particle velocity, which is

$$V_{\text{incident}} = \frac{A_n}{Y_n} \quad (28)$$

By re-arranging Eq. (20) the total pressure at the inlet is

$$p_n = \frac{E_{12}}{E_{22}} \times V_n \quad (29)$$

After some algebraic manipulation (using Mathcad) it can be shown that the total inlet pressure is

$$p_n = \frac{2E_{12}Y_n}{E_{12} + E_{22}Y_n} \times V_{\text{incident}} \quad (30)$$

and the corresponding total inlet velocity is

$$V_n = \frac{2E_{22}Y_n}{E_{12} + E_{22}Y_n} \times V_{\text{incident}} \quad (31)$$

Eqs. (29) and (30) can be used to calculate the inlet total pressure and velocity, and can then be used in Eq. (20) to calculate the outlet velocity, and Eq. (25) to calculate the outlet pressure.

The transmission loss is calculated as (Munjal (1987), p82, Eq. (2.150))

$$\text{TL}=20\log_{10}\left[\left\{\frac{Y_1}{Y_n}\right\}^{\frac{1}{2}} \times \left|\frac{T_{11} + \frac{T_{12}}{Y_1} + Y_n T_{21} + \left(\frac{Y_n}{Y_1}\right) T_{22}}{2}\right|\right] \quad (32)$$

and can be modified to account for the different speed of sound and cross sectional areas at the inlet and outlet as

$$\text{TL} = 20\log_{10}\left[\left\{\frac{c_1}{S_1}\frac{S_n}{c_n}\right\}^{\frac{1}{2}} \times \left|\frac{T_{11} + T_{12}\frac{S_1}{c_1} + \frac{c_n}{S_n}T_{21} + \left(\frac{c_n}{S_n}\frac{S_1}{c_1}\right) T_{22}}{2}\right|\right] \quad (33)$$

where $c_1$is the speed of sound at the outlet of the duct network and $S_1$is the cross sectional area of the duct outlet. Similarly $c_n$ is the speed of sound at the inlet of the duct and $S_n$is the cross sectional area.

An example application of these equations will be shown where a quarter-wave tube is installed in a duct with applied temperature gradients. Table 1 lists the dimensions of an example duct network used to compare theoretical predictions implemented in Matlab, with results from finite element analyses conducted using Ansys.

**Table 1**. Parameters used for example system.

| Description | Parameter | Value | Units |
|---|---|---|---|
| Radius of all ducts | $a$ | 0.05 | m |
| Length of upstream duct | $L_{\text{upstream}}$ | 1.0 | m |
| Length of downstream duct | $L_{\text{downstream}}$ | 1.0 | m |
| Length of QWT | $L_{\text{QWT}}$ | 1.0 | m |
| Gas temperature at duct inlet | $T_{\text{inlet}}$ | 500 | °C |
| Gas temperature at junction to QWT | $T_{\text{QWT inlet}}$ | 400 | °C |
| Gas temperature at rigid end of QWT | $T_{\text{QWT end}}$ | 100 | °C |
| Gas temperature at duct outlet | $T_{\text{outlet}}$ | 300 | °C |
| Incident acoustic particle velocity at duct inlet | $u_{\text{inlet}}$ | 1.0 | m/s |

## FINITE ELEMENT MODEL

The process for conducting an acoustic finite element analysis where there are variations in the temperature of the gas involves several steps as follows:

1. A solid model is created that defines the geometry of the system.
2. The solid model is meshed with thermal elements (SOLID70).
3. The temperature boundary conditions are applied for each region.
4. A static thermal analysis is conducted to calculate the temperature distribution of the nodes throughout the duct network.
5. The temperatures at each node are stored in an array.
6. The thermal elements are replaced with acoustic elements (FLUID30).
7. The values of temperatures stored in the array are used to define the temperature at each node of the acoustic elements.
8. Anechoic boundary conditions are set at the duct inlet and outlet (using the MAPDL command SF,nodes,IMPD,INF).
9. The acoustic velocity at the duct inlet is defined (using the MAPDL command SF,nodes,SHLD,velocity).
10. A harmonic analysis is conducted over the analysis frequency range.
11. The sound pressure levels at the duct inlet, outlet, and the entrance and closed end of the QWT are calculated.

Figure 7 shows the finite element model created in Ansys, where the red ends indicate the anechoic terminations.

Figure 8 shows the temperature profile in the duct network, where the temperature at the inlet to the duct (right side of figure) was 500°C=773K, at the outlet of the main duct was 300°C=573K, and at the closed end of the QWT was 100°C=373K. It is assumed in the one-dimensional mathematical model that the temperature at the junction between the main duct and the entrance to the QWT is constant at 400°C=673K. However the temperature field in this region calculated using the 3-dimensional finite element model has a small variation, as shown in Figure 9.

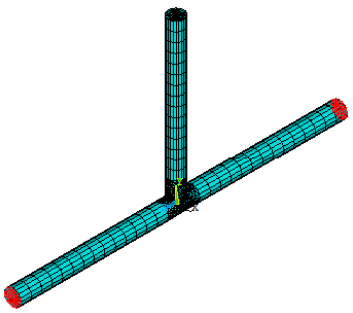

**Figure 7**. Finite element model of the duct network.

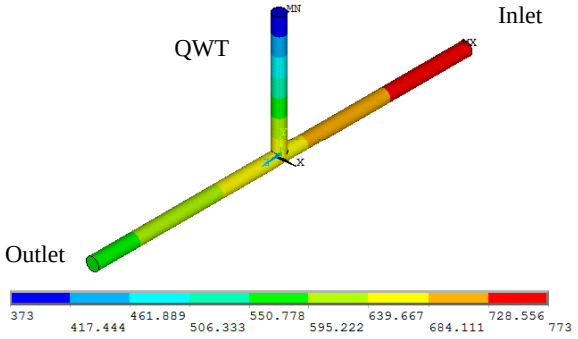


**Figure 8.** Finite element results of the temperature distribution in the duct, where the colour contours are in units of Kelvin.

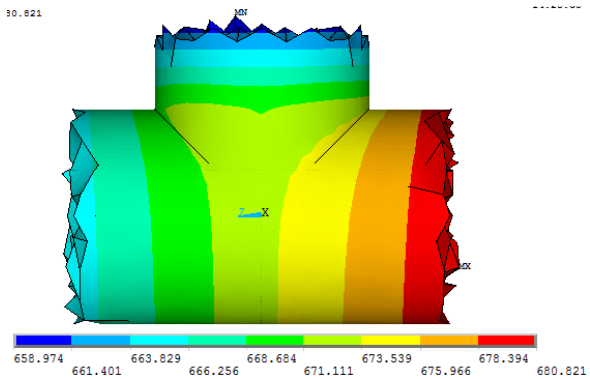


**Figure 9.** Temperature contour plot at the junction between the main duct and the entrance to the QWT, where the colour contours are in units of Kelvin.

## COMPARISON OF RESULTS

This section contains comparisons of predictions of several acoustic parameters calculated using the theoretical model described in this paper and calculated using Ansys.

Figure 10 shows the sound pressure level at the inlet and outlet of the duct with and without the QWT and with the applied temperature gradient, calculated using the theoretical model and using Ansys. It can be seen that the Ansys results (shown as the dots) overlay the theoretical predictions. The minimum sound pressure level at the anechoic outlet of the duct occurs at 126Hz.

Figure 11 and Figure 12 show the real and imaginary parts of the mass volume velocity in the duct with the applied temperature gradients calculated using the theoretical model and using Ansys, without and with the QWT, respectively. It can be seen that the results calculated using Ansys overlay the theoretical predictions. A subtle result from these analyses is that the inlet mass volume velocity varies across the analysis frequency range and is not constant. The theoretical and Ansys analyses used a constant *incident* inlet acoustic particle velocity. The results shown in the figures are the total mass volume velocities, which is the sum of the incident and reflected velocities and varies across the analysis frequency range.

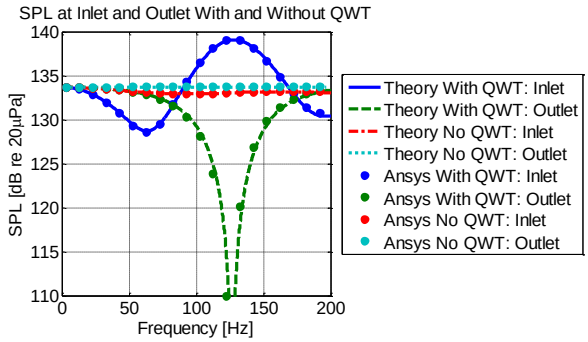


**Figure 10.** Sound pressure levels in the duct with a gas temperature gradient, with and without a QWT, calculated using a theoretical model and using Ansys.

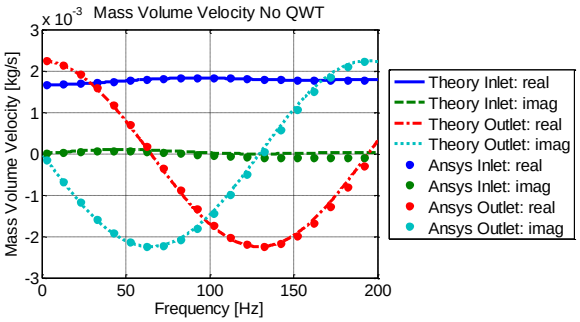


**Figure 11.** Mass volume velocity in duct without QWT, calculated using a theoretical model and using Ansys.

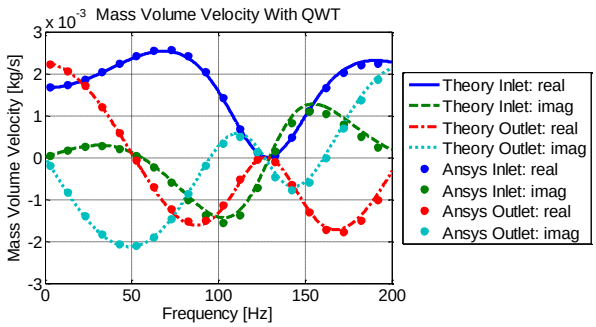


**Figure 12.** Mass volume velocity in duct with QWT, calculated using a theoretical model and using Ansys.

Figure 13 shows the transmission loss in the duct without and with the QWT. Transmission loss is the difference in the incident sound power and the transmitted sound power at the outlet calculated using the theoretical model. As shown in the previous figures, the Ansys results for pressure and mass volume velocity overlayed the theoretical predictions, and as transmission loss is derived from these quantities, it follows that the calculated transmission loss using Ansys results also overlay theoretical predictions. The figure shows that the highest transmission loss occurs at 126Hz. The transmission loss results were calculated by two methods: (1) using the division of the elements of the transmission matrix model

shown in Eq. (33) and is labelled '4 pole', and (2) by calculating the acoustic power from using the incident acoustic pressure and volume velocities at the inlet and the transmitted acoustic pressure and volume velocities at the outlet and is labelled $\Delta L_w$. It can be seen that these results from the different prediction methods overlay each other, which is to be expected.

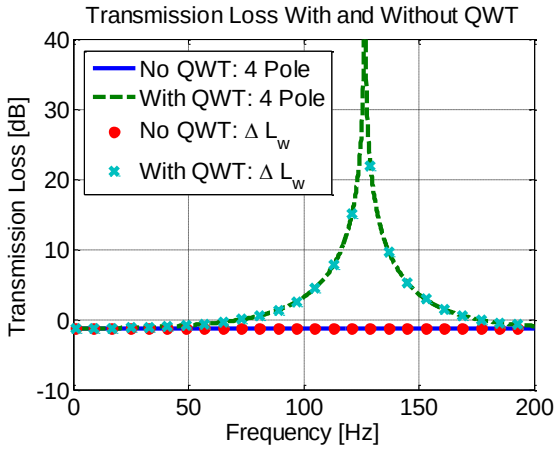


**Figure 13.** Transmission loss in a duct with and without a QWT, calculated using a theoretical model.

## CONCLUSION

This paper presented equations for the transmission matrix model of a duct with a quarter-wave tube where a linear temperature occurs in the gas between the inlet and outlet of the duct and along the quarter-wave tube. The theoretical model was compared with predictions using finite element analysis using the software Ansys, that has introduced a new capability for temperature gradients in acoustic elements. It was shown that when specifying an incident acoustic velocity as the excitation source into the duct, some adjustments to the formulation of the four pole transmission matrix are necessary.

## REFERENCES

Bies, D.A. and Hansen, C.H. 2009, *Engineering Noise Control: Theory and Practice*, 4th edition, Spon Press, Abingdon, UK.

Beranek, L. L. and Ver, I.L. (1992), "Noise and Vibration Control Engineering: Principles and Applications", John Wiley and Sons, New York, USA, ISBN: 0471617512, page 377.

Howard, C.Q. (2013), "The corrected expressions for the four-pole transmission matrix for a duct with a linear temperature gradient and an exponential temperature profile ", *The Open Journal of Acoustics*, vol. 3, no. 3, In Press.

Munjal, M. L. and Prasad, M. G. (1986), "On plane-wave propagation in a uniform pipe in the presence of a mean flow and a temperature gradient", *The Journal of the Acoustical Society of America*, vol 80, no 5, p1501-1506.

Munjal, M.L. (1987), "Acoustics of Ducts and Mufflers: With Application to Exhaust and Ventilation System Design", John Wiley and Sons. 352 pages. ISBN: 978-0-471-84738-0.

Peat, K.S. (1988), "The transfer matrix of a uniform duct with a linear temperature gradient", *Journal of Sound and Vibration*, vol 123, no 1, pp 45-53.

Sujith, R. I., Waldherr, G. A., and Zinn, B. T. (1985), ''Exact Solution for Sound Propagation in Ducts with Axial Temperature Gradient,'' *Journal of Sound and Vibration*, Vol. 184, pp 389–402.

Sujith, R. I. (1996), "Transfer matrix of a uniform duct with an axial mean temperature gradient", *The Journal of the Acoustical Society of America*, vol 100, no. 4, pp2540-2542.